General and Comparative Endocrinology 284 (2019) 113234

Contents lists available at ScienceDirect

General and Comparative Endocrinology

journal homepage: www.elsevier.com/locate/ygcen

Orange-spotted grouper melanocortin-4 receptor: Modulation of signaling by MRAP2

Ying-Zhu Rao[a,b], Rong Chen[a], Yong Zhang[c], Ya-Xiong Tao[b,*]

[a] Institute of Applied Biotechnology, Life Science and Technology School, Lingnan Normal University, Zhanjiang 524048, Guangdong, China
[b] Department of Anatomy, Physiology and Pharmacology, College of Veterinary Medicine, Auburn University, Auburn, AL 36849, United States
[c] Laboratory for Marine Fisheries Science and Food Production Processes, Qingdao National Laboratory for Marine Science and Technology, Qingdao 266373, China

ARTICLE INFO

Keywords:
Orange-spotted grouper
Epinephelus coioides
Melanocortin-4 receptor
Melanocortin receptor accessory protein 2
Tissues distribution
Pharmacology

ABSTRACT

Melanocortin-4 receptor (MC4R) and melanocortin receptor accessory protein 2 (MRAP2) play important roles in the melanocortin system, and interaction of MC4R and MRAP2 is suggested to play pivotal role in energy balance of vertebrates. Orange-spotted grouper (*Epinephelus coioides*) is a widely cultured marine fish with high economic value in Asia. To explore potential interaction between grouper MC4R and MRAP2, herein we cloned grouper *mc4r* and *mrap2*. Grouper *mc4r* consisted of a 981 bp ORF encoding a putative protein of 327 amino acids, while the grouper *mrap2* consisted of a 696 bp ORF encoding a putative protein of 232 amino acids. Sequence and phylogenetic analysis revealed that the grouper MC4R and MRAP2 were highly homologous at amino acid levels to several teleost MC4Rs and MRAP2s, respectively. qRT-PCR results showed that both *mc4r* and *mrap2* were expressed primarily in the central nervous system. In the periphery, these genes were expressed more widely in male fish. The cloned grouper MC4R was functional, exhibiting high constitutive activity in cAMP pathway, capable of binding to three peptide agonists and increasing intracellular cAMP production dose-dependently. MRAP2 significantly decreased basal and agonist-stimulated cAMP signaling. MRAP2 also increased basal ERK1/2 activation but decreased ligand-induced stimulation when expressed at high levels. These data will facilitate future investigation of these molecules in regulating diverse physiological processes in orange-spotted grouper.

1. Introduction

The melanocortin-4 receptor (MC4R) (Gantz et al., 1993; Mountjoy et al., 1994), one of the five subtypes of melanocortin receptors (MCRs), is highly expressed in the central nervous system, constituting an important component of the central melanocortin system. It regulates diverse physiological processes including energy homeostasis, reproduction and sexual function (reviewed in (Tao and Segaloff, 2005; Tao, 2010)). Loss of *Mc4r* in mice results in increased food intake, decreased energy expenditure and morbid obesity (Huszar et al., 1997; Balthasar et al., 2005). Mutations in *MC4R* are the most prevalent form of human monogenic obesity, implicated in up to 6% of early onset severe obesity cases (Farooqi et al., 2003; Tao, 2009; Hinney et al., 2013).

As a member of Family A G protein-coupled receptors (GPCRs), MC4R is coupled to Gs, increasing intracellular cAMP level upon receptor activation. In addition, the MC4R also activates mitogen-activated protein kinase (MAPK), especially extracellular signal-regulated kinase 1 and 2 (ERK1/2) (Daniels et al., 2003; Vongs et al., 2004; Sutton et al., 2005; Huang and Tao, 2012; Mo et al., 2012). Biased signaling among these two pathways has also been observed (Nickolls et al., 2005; Breit et al., 2006; Mo and Tao, 2013) (reviewed in (Yang and Tao, 2017)). For example, we showed that some naturally occurring mutations in the *MC4R* result in mutant receptors with normal Gs-cAMP signaling but altered basal and ligand-stimulated ERK1/2 signaling (He and Tao, 2014).

Melanocortin-2 receptor accessory protein (MRAP) was identified as receptor-specific molecular chaperone, essential for trafficking melanocortin-2 receptor (MC2R) to the plasma membrane (Metherell et al., 2005). Subsequently, another MRAP, MRAP2, was identified (Sebag and Hinkle, 2007). MRAPs are small proteins with a single transmembrane domain. In vitro studies showed that MRAP2 interacts with all five MCRs, exerting different effects on receptor expression, binding and signaling (Metherell et al., 2005; Chan et al., 2009; Sebag and Hinkle, 2009a; Sebag and Hinkle, 2010; Asai et al., 2013; Novoselova et al., 2016).

* Corresponding author.
E-mail address: taoyaxi@auburn.edu (Y.-X. Tao).

https://doi.org/10.1016/j.ygcen.2019.113234
Received 17 February 2019; Received in revised form 2 July 2019; Accepted 28 July 2019
Available online 06 August 2019
0016-6480/

Table 1
Primers used for cDNA cloning and qPCR.

Primer name	Primer sequence (5′–3′)	Purpose	Product size (bp)
MC4R-F	ATGAACACCACAGAGAACCATGGATTGAT	MC4R ORF PCR	984
MC4R-R	TCACACACACAACAGAGTGTGCGAGCAGC	MC4R ORF PCR	
MRAP2-F	ATGTCCGACTTCCACAACCGGAGCCA	MRAP2 ORF PCR	699
MRAP2-R	TTAGCGGATGTCACAGTGAGCATCCT	MRAP2 ORF PCR	
MC4R-qF	GGCATCTTGTTCATCATTTACTCAG	MC4R qPCR	100
MC4R-qR	GGACGTACAGTGACGCCATG	MC4R qPCR	
MRAP2-qF	TAGAGGAGGGTAAGACCGACAG	MRAP2 qPCR	119
MRAP2-qR	GGACGGCTCATACAGCAGAT	MRAP2 qPCR	
Actin-qF	TGTCCCTGTATGCCTCTGGTC	β-Actin qPCR	
Actin-qR	TGATGTCACGCACGATTTCC	β-Actin qPCR	
GAPDH-qF	GACACCCACTCCTCCATCTTT	GAPDH qPCR	102
GAPDH-qR	GTTGCTGTATCCGAACTCGTT	GAPDH qPCR	

β-actin and *gapdh* were used as housekeeping genes.

With human MC4R, MRAP2 has no effect on basal signaling but decreases agonist-stimulated signaling (Chan et al., 2009). In mouse MC4R, MRAP2 decreases basal signaling but increases maximal response to agonist stimulation (Asai et al., 2013). Therefore, MRAP2 has different effects on human and mouse MC4R signaling. Rare potentially pathogenic variants in *MRAP2* were identified to be associated with severe early-onset obesity (Asai et al., 2013). In mice, whole body and brain-specific deletion of *Mrap2* leads to severe obesity at a young age (Asai et al., 2013). These studies demonstrated that MRAP2 plays a key role in MC4R signaling and body weight regulation in mammals (Asai et al., 2013; Sebag et al., 2013).

MC4R has been studied in several fishes (Cerda-Reverter et al., 2003; Song and Cone, 2007; Sebag et al., 2013; Wei et al., 2013; Li et al., 2016; Li et al., 2017; Yi et al., 2018). MRAP2 has also been identified from several cartilaginous and teleost fishes, with some fishes only having MRAP2 but not MRAP1 (Västermark and Schiöth, 2011; Valsalan et al., 2013). Potential interaction between MC4R and MRAPs in fish has only been studied in zebrafish, which has two MRAP2s, MRAP2a and MRAP2b (Josep Agulleiro et al., 2013; Sebag et al., 2013). In adult zebrafish, MC4R and MRAP2 are co-expressed in some areas of central nervous system. *In vitro* studies showed that MRAP2a decrease the ability of zebrafish MC4R to bind α-MSH, while MRAP2b increases ligand sensitivity (Josep Agulleiro et al., 2013; Sebag et al., 2013). *mrap2a* and *mrap2b* are expressed at different stages of zebrafish development: the larval form, MRAP2a, stimulates growth by antagonizing MC4R action whereas the adult form, MRAP2b, potentiates MC4R action (Sebag et al., 2013). Therefore, it is important to reveal the interaction between MRAP2 and MC4R in fish. Comparative analysis of the MC2R pharmacology and requirement for its expression on the cell surface lead to the hypothesis that the ligands (derived from tissue-specific post-translational processing of POMC), the MC2R-specific chaperone – MRAP, and the MCRs, co-evolved (Dores and Garcia, 2015).

The orange-spotted grouper, *Epinephelus coioides*, belonging to family Serranidae, is an economically important marine teleost distributed in the tropics and subtropics and widely cultured in China and other Asian countries (Chen et al., 2008). Low larval survival rate and slow fingerling growth rate are major challenges in grouper culture (Wang et al., 2014). It is of significant interest to gain a better understanding of the regulation of energy balance in grouper. To explore the potential interaction between MC4R and MRAPs, and their roles in energy balance and reproduction of orange-spotted grouper, we analyzed our transcriptome and genome databases. We showed that grouper had one copy of *mrap2* but did not have *mrap1*. We also identified grouper *mc4r* and studied the tissue distribution of *mrap2* and *mc4r*. The pharmacological properties of grouper MC4R (*Eco*MC4R) and the modulation by MRAP2 were investigated.

2. Materials and methods

2.1. Ligands and plasmids

[Nle^4, D-Phe^7]-α-melanocyte stimulation hormone (NDP-MSH) was purchased from Peptides International (Louisville, KY, USA), human α-MSH from Pi Proteomics (Huntsville, AL, USA) and ACTH (1–24) from Phoenix Pharmaceuticals (Burlingame, CA, USA). Grouper POMC has been cloned previously (Zhang et al., 2003). It showed that grouper α-MSH is 100% conserved with human α-MSH, whereas there are only two amino acids different between human and grouper ACTH(1–24). Therefore human peptides are appropriate for use in this study. [^{125}I]-NDP-MSH and [^{125}I]-cAMP were iodinated in our lab using chloramine T method as previously described (Steiner et al., 1969; Mo et al., 2012). The N-terminal c-myc-tagged human MC4R (hMC4R) subcloned into pcDNA3.1 was generated as previously described (Tao and Segaloff, 2003).

2.2. Molecular cloning of EcoMC4R and EcoMRAP2

Total RNA was extracted from grouper brain using Total RNA Extractor Trizol reagent (Sangon, Shanghai, China), treated with DNase, and reverse transcribed using PrimeScript™ II 1st Strand cDNA Synthesis Kit (Takara, Beijing, China). The primers were designed based on the *mc4r* and *mrap2* sequences we identified (Table 1). PCR products were separated by 1.2% agarose gel electrophoresis, purified by SanPrep Column DNA Gel Extraction Kit (Sangon), ligated into pMD18-T (Takara, Beijing, China), and transformed into DH5α for sequencing. The verified coding sequence of *mc4r* and *mrap2* were then synthesized by PCR and subcloned into pcDNA3.1 vector by GenScript (Piscataway, NJ, USA). The nucleotide sequences of the cloned grouper *mc4r* and *mrap2* were deposited in GenBank with accession numbers MH888335 and MK425026, respectively. All animal experiments were conducted in accordance with the guidelines and approval of the Animal Research and Ethics Committee of Sun Yat-sen University.

2.3. Homology and phylogenetic analyses of EcoMC4R and EcoMRAP2

The putative TMDs of *Eco*MC4R were predicted based on the crystal structure of rhodopsin (Palczewski et al., 2000) and that reported for hMC4R (Tao, 2010). The multiple alignments of amino acid sequences from different species and homology analysis were performed with Clustal Omega online program (http://www.ebi.ac.uk/Tools/msa/clustalo/). The phylogenetic trees of *Eco*MC4R and *Eco*MRAP2 were constructed with 1000 bootstrap replications using the neighbor-joining (NJ) method (Saitou and Nei, 1987) and MEGA 6.0 software.

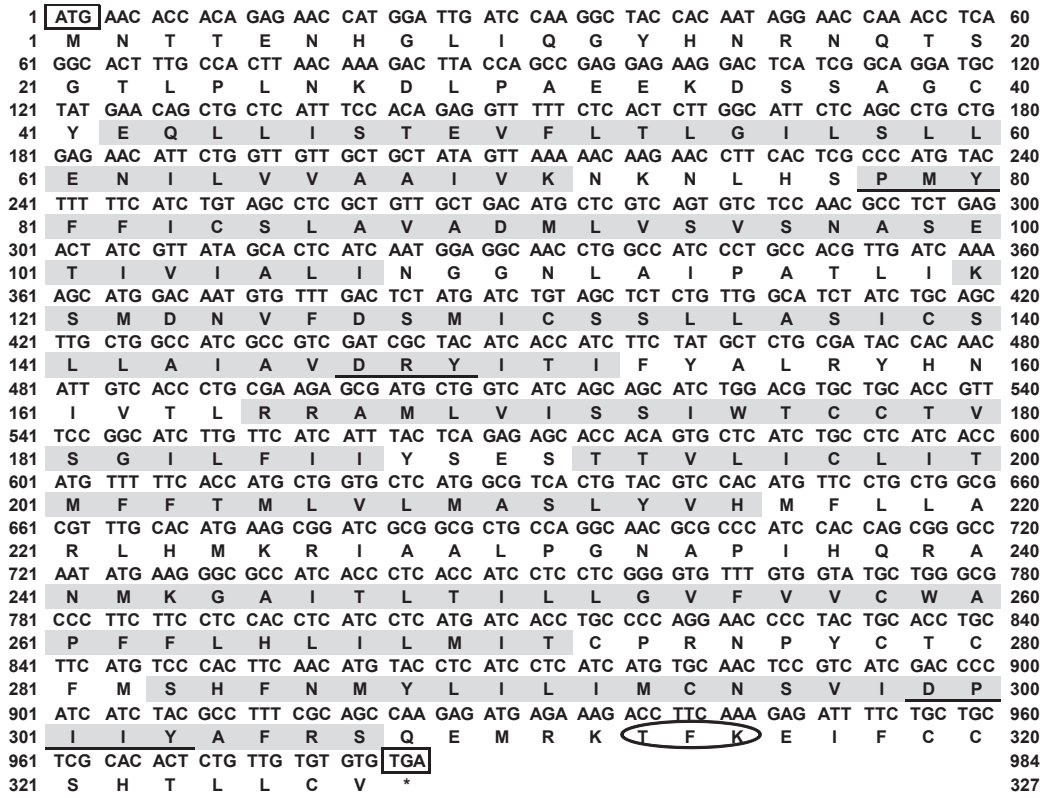

Fig. 1. Nucleotide and deduced amino acid sequence of *Eco*MC4R. Positions of nucleotide and amino acid sequences are indicated on both sides. Amino acids in shaded boxes indicate putative transmembrane domains. Oval frames enclose potential phosphorylation sites. PMY, DRY, DPxxY motifs are underlined. Open boxes show initiation codon and stop codon. Asterisk (*) denotes stop codon.

2.4. Quantitative real-time PCR (qRT-PCR) for tissue distribution

To investigate tissue distribution of the two genes, the following tissues (olfactory bulb, cerebrum, mesencephalon, cerebellum, medulla, hypothalamus, pituitary gland, heart, liver, intestine, stomach, gonads, head kidney, kidney, skin, muscle, gill and spleen) were taken from six male and six female adults (60 cm body length and 4 kg body weight on average), respectively. The geometric mean of the expression of two reference genes, *β-actin* and *gapdh* (*glyceraldehyde-3-phosphate dehydrogenase*), were used as the control (Bustin et al., 2009). The primers used were listed in Table 1. The cDNA was synthesized using Transcriptor First Strand cDNA Synthesis Kit (Roche) and then stored at −20 °C. The qRT-PCR amplifications were carried out using LightCycler® 480 SYBR® Green I Master (Roche) on a LightCycle 480 system. The qRT-PCR profiles included an initial denaturation step at 95 °C for 2 min, followed by 45 cycles of 95 °C for 10 sec, 55 °C for 15 sec and 72 °C for 20 sec. Dissociation curve analysis was performed following each PCR reaction to confirm that only one target product was amplified. All reactions were performed in duplicate. The results obtained were normalized as the fold of pituitary expression and the relative expression levels in different tissues were calculated via the comparative CT method ($2^{-\triangle\triangle CT}$) (Livak and Schmittgen, 2001). All data were expressed as the mean ± SEM (n = 6).

2.5. Cell culture and transfection

To investigate the ligand binding and signaling properties of *Eco*MC4R, three ligand of the MC4R, NDP-MSH, α-MSH, and ACTH (1–24), were used. Human embryonic kidney (HEK) 293 T cells (ATCC, Manassas, VA, USA) were cultured in Dulbecco's Modified Eagle's medium (DMEM) (Invitrogen, Carlsbad, CA, USA) containing 10% newborn calf serum (PAA Laboratories, Etobicoke, ON, Canada), 10 mM HEPES, 0.25 μg/ml of amphotericin B, 50 μg/ml of gentamicin, 100 IU/ml of penicillin, and 100 μg/ml of streptomycin at 37 °C in a 5% CO_2-humidified atmosphere. The HEK cells were plated into 6-wells plates (Corning, Corning, NY, USA) pre-coated with 0.1% gelatin. At approximately 50–70% confluence, the cells were transfected with MC4R plasmids with or without MRAP2 using calcium phosphate precipitation method (Chen and Okayama, 1987).

2.6. Ligand binding assays

Binding assay was performed as described previously (Tao and Segaloff, 2003). The final concentrations of unlabeled ligands for competition with radio-labeled NDP-MSH were 10^{-11} to 10^{-6} M for NDP-MSH, 10^{-10} to 10^{-5} M for α-MSH and ACTH (1–24). The radioactivity was counted by a gamma counter (Cobra II Auto-Gamma, Packard Bioscience, Frankfurt, Germany). All determinations were performed in duplicate, and each experiment was performed at least three times independently.

2.7. Ligand-stimulated cAMP accumulation assays

cAMP signaling assay was performed as described previously (Tao and Segaloff, 2003). The final concentrations of ligands used were 10^{-12} M to 10^{-6} M for NDP-MSH and ACTH (1–24), 10^{-11} M to 10^{-5} M for α-MSH. The cAMP concentrations were determined by radioimmunoassay as previously described (Steiner et al., 1969; Tao, 2010). All determinations were performed in triplicate, and each experiment was performed at least three times independently.

To investigate potential modulation of MRAP2 on MC4R signaling, cells were co-transfected with MC4R and MRAP2 plasmids at different ratios of 1:0, 1:1, 1:3 and 1:5. Empty vector pcDNA3.1 was added so that all groups were transfected with the same amount of DNA. The

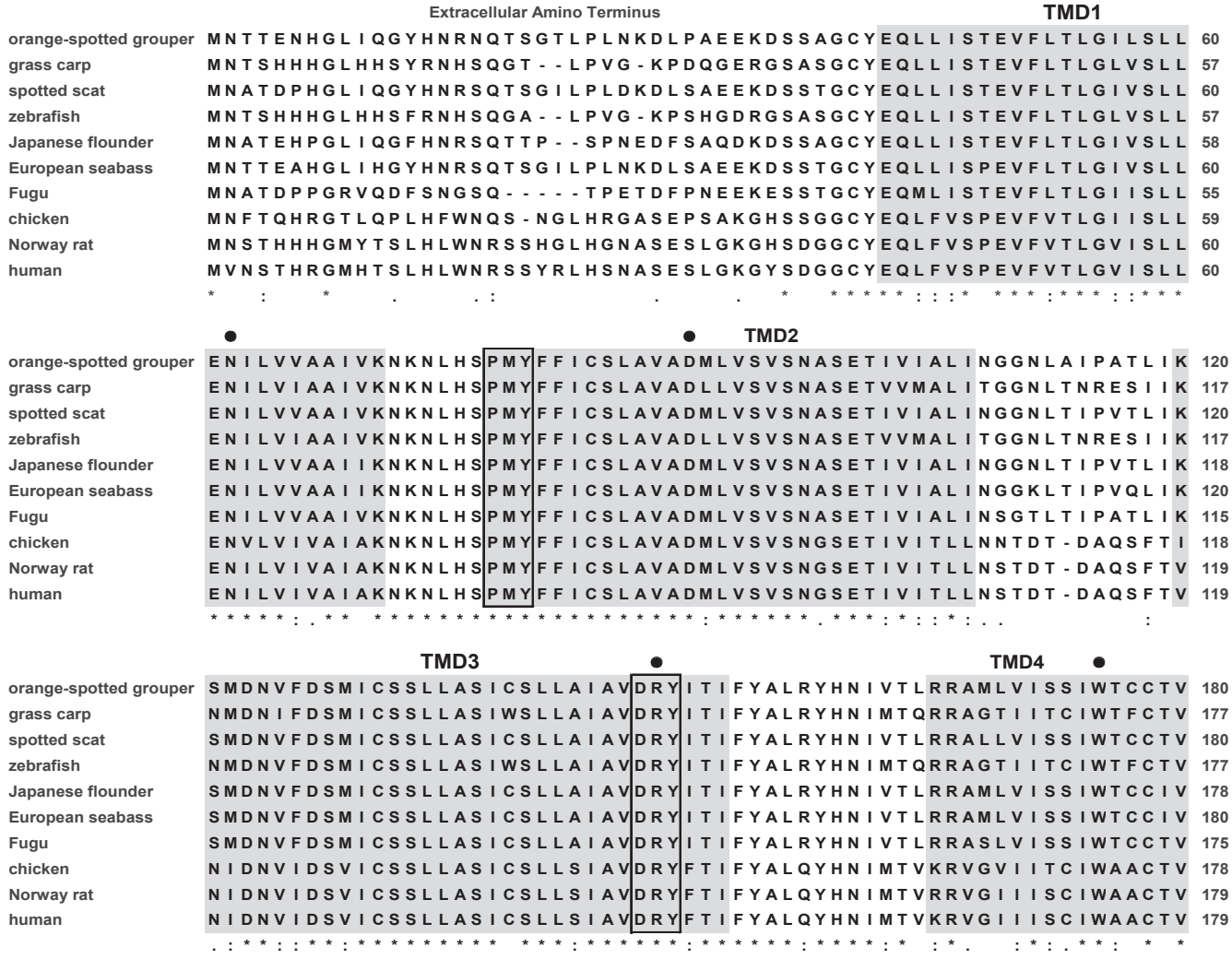

Fig. 2. Comparison of amino acid sequences between *Eco*MC4R and MC4Rs from other species. Transmembrane domains are shown in shaded boxes as TMD 1–7. Amino and carboxyl termini show as extracellular amino terminus and cytoplasmic tail, respectively. PMY, DRY, DPxxY motifs are shown by open boxes. Predicted phosphorylation sites are shown by dark shadow. The most conserved residues in each TMD are indicated by black dots. The potential palmitoylation sites at the C termini are indicated by black arrowheads. Asterisk (*) indicates the same amino acids. MC4Rs: *Epinephelus coioides* (orange-spotted grouper, MH888335), *Ctenopharyngodon idella* (grass carp, AOZ60534.1), *Scatophagus argus* (spotted scat, KU760724.1), *Danio rerio* (zebrafish, NP_775385.1), *Paralichthys olivaceus* (Japanese flounder, ADP09415.1), *Dicentrarchus labrax* (European sea bass, CBN82190.1), *Takifugu rubripes* (fugu, NP_001027732.1), *Gallus gallus* (chicken, AEP17334.1), *Rattus norvegicus* (Norway rat, NP_037231.1), and *Homo sapiens* (human, NP_005903.2).

cAMP assay was carried out as described above.

2.8. ERK1/2 phosphorylation assay

We also evaluated the potential effect of MRAP2 on ERK1/2 signaling stimulated by *Eco*MC4R. At approximately 50–70% confluency, cells were co-transfected with grouper MC4R and MRAP2 at different plasmid ratios (1:0, 1:1, 1:3 and 1:5). 24 h after transfection, cells were washed twice with DMEM/BSA and starved in DMEM/BSA for 24 h. Then cells were treated for 5 min at 37 °C with either buffer alone or 10^{-6} M α-MSH. The ERK1/2 phosphorylation was measured as described previously (Huang and Tao, 2012; Mo et al., 2012). Films developed were quantified using ImageJ 1.44 software (National Institute of Health, Bethesda, MD). ERK1/2 phosphorylation was normalized by expressing the data as a ratio of pERK1/2 over β-tubulin from the same gel.

2.9. Statistical analysis

GraphPad Prism 7.0 software (San Diego, CA, USA) was used to calculate the parameters of ligand binding and cAMP signaling assays. The significance of differences in expression levels, ligand binding and cAMP signaling parameters between *Eco*MC4R and hMC4R, as well as vehicle and ligand-treated groups, were all determined by Student's *t*-test. ANOVA method was used to analysis the significance of differences in cAMP and ERK1/2 signaling after co-transfection of MC4R and MRAP2.

3. Results

3.1. Nucleotide and deduced amino acid sequences of EcoMC4R and EcoMRAP2

The cloned grouper *mc4r* cDNA contained an open reading frame of 981 bp, encoding a putative protein of 327 amino acids with an estimated molecular mass of 36.54 kDa (Fig. 1). The *Eco*MC4R consisted of seven putative hydrophobic TMDs connected by alternating extracellular (ECL) and intracellular (ICL) loops with an extracellular N-terminus and an intracellular C-terminus (Figs. 1 and 2). The deduced amino acid sequence was significantly conserved in the TMDs,

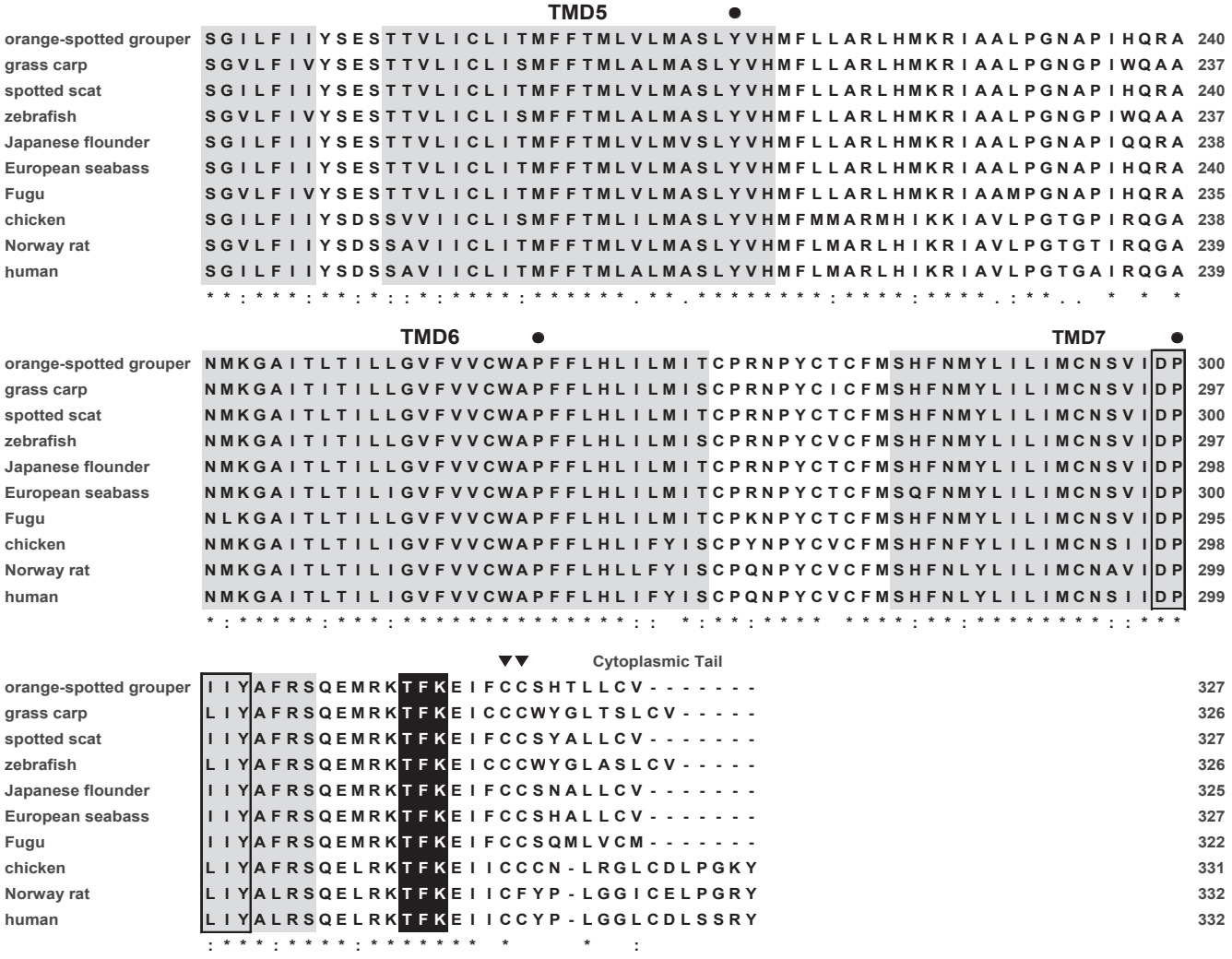

Fig. 2. (*continued*)

```
1   ATG TCC GAC TTC CAC AAC CGG AGC CAA ACC AGC GCA CGT CGC AGT GAC TAC GTG TGG CAG 60
1   M   S   D   F   H   N   R   S   Q   T   S   A   R   R   S   D   Y   V   W   Q   20
61  TAT GAA TAT TAC GAC GAT GAG GAG CCC GTG TCG TTT GAG GGA CTC AAA GCG CAC AGA TAC 120
21  Y   E   Y   Y   D   D   E   E   P   V   S   F   E   G   L   K   A   H   R   Y   40
121 TCC ATC GTC ATC GGC TTC TGG GTC GGA CTT GCT GTG TTT GTC ATT TTC ATG TTC TTT GTT 180
41  S   I   V   I   G   F   W   V   G   L   A   V   F   V   I   F   M   F   F   V   60
181 CTC ACG CTG CTC ACA AAG ACA GGA GCG CCA CAT CAA GAA AAC CCA GAC TCT GCT GAA AAG 240
61  L   T   L   L   T   K   T   G   A   P   H   Q   E   N   P   D   S   A   E   K   80
241 CGC CAT CGA CCA GGC AGC TGT CTG GTA GAC ATC GGC AGC CCC CAG GAC GAA AAT GAC AAA 300
81  R   H   R   P   G   S   C   L   V   D   I   G   S   P   Q   D   E   N   D   K   100
301 GCC TTT TCT CGC CCT CTG CTA GCC GAG TCC CGC TCT TAT TTT CAT TTC TAC ATC AAC GAG 360
101 A   F   S   R   P   L   L   A   E   S   R   S   Y   F   H   F   Y   I   N   E   120
361 GAG GAT CAG GGT CAG GGG AAG CAA AAA CCA GGG GAC GAG AGG GTC GGA AAG CAC TGC GGG 420
121 E   D   Q   G   Q   G   K   Q   K   P   G   D   E   R   V   G   K   H   C   G   140
421 GCT CGT GGC CAG CAG GGG ACC AGA GGT ATC AGC TCG TCT GGG ATG ATG GAC GAG ATG GAA 480
141 A   R   G   Q   Q   G   T   R   G   I   S   S   S   G   M   M   D   E   M   E   160
481 GAG GAC GCC GAG GAA GCT CGG GGA CAC CAA CCT CTC AAG GGA CTA ATA GAG GAG GGT AAG 540
161 E   D   A   E   E   A   R   G   H   Q   P   L   K   G   L   I   E   E   G   K   180
541 ACC GAC AGA GAA TGT GCC TTC TTT TCC CAC TTC AAC ATC CCT AAC TTT GTG AAC TTG GAG 600
181 T   D   R   E   C   A   F   F   S   H   F   N   I   P   N   F   V   N   L   E   200
601 CAC AGT TCG ACA CTC GGA GAG GAT GAT CTG CTG TAT GAG CCG TCC GCC ATC CTG GAG CGC 660
201 H   S   S   T   L   G   E   D   D   L   L   Y   E   P   S   A   I   L   E   R   220
661 CAG TCT CAC TCT CAG GAT GCT CAC TGT GAC ATC CGC TAA                             699
221 Q   S   H   S   Q   D   A   H   C   D   I   R   *                             232
```

Fig. 3. Nucleotide and deduced amino acid sequence of *Eco*MRAP2. Positions of nucleotide and amino acid sequences are indicated on both sides. Amino acids in shaded box indicate putative transmembrane domain. Open box shows putative *N*-linked glycosylation sites. Initiation codon and stop codon are underlined. Asterisk (*) denotes stop codon.

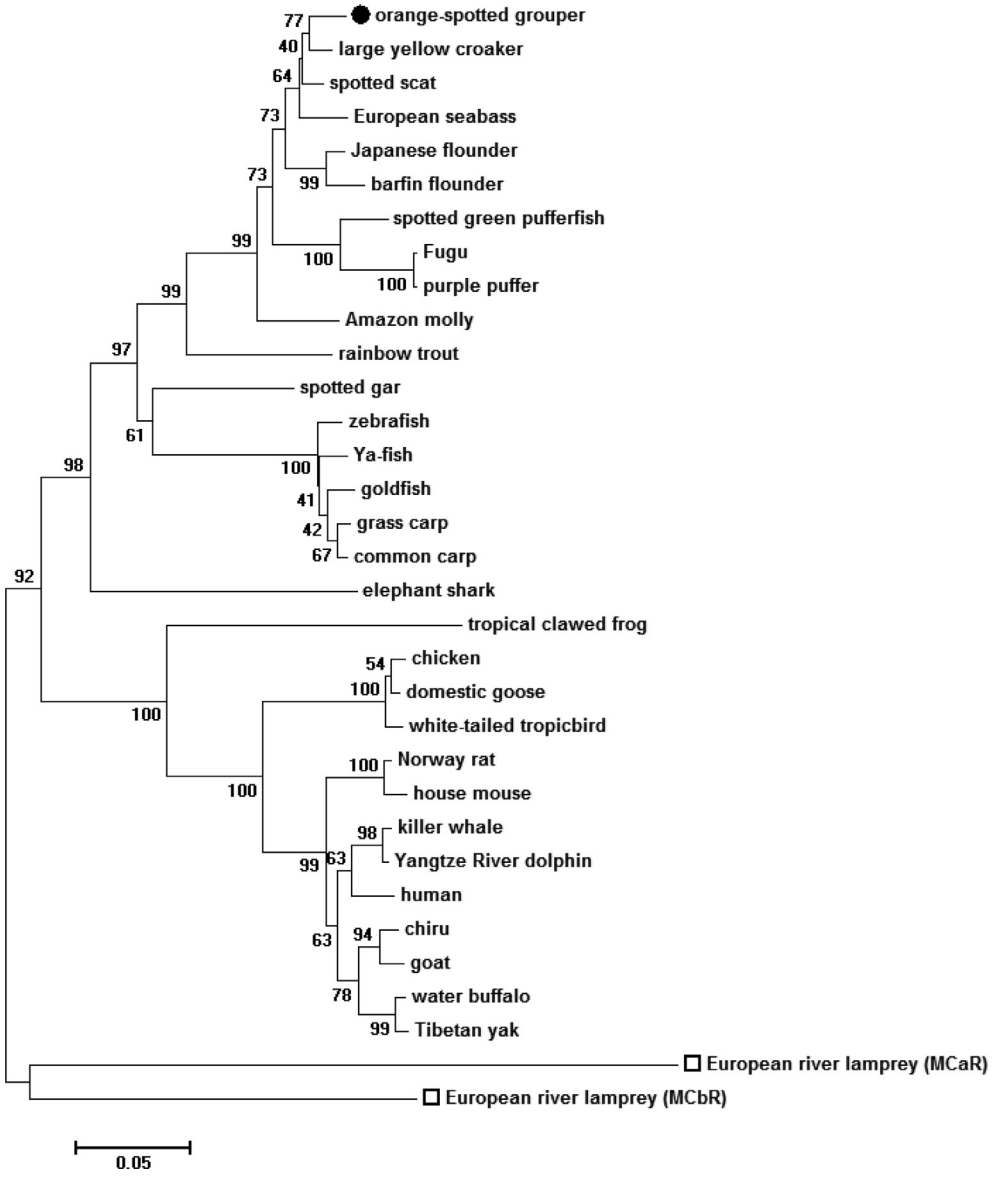

Fig. 4. Phylogenetic tree of MC4Rs. The tree was constructed using the neighbor-joining (NJ) method. Numbers at nodes indicate the bootstrap value, as percentages, obtained for 1000 replicates. Black dot and open boxes shows *Eco*MC4R and outgroup, respectively. MC4Rs: *Epinephelus coioides* (orange-spotted grouper, MH888335), *Lampetra fluviatilis* (European river lamprey, MCaR: ABB36647.1, and MCbR: ABB36648.1), *Callorhinchus milii* (elephant shark, XP_007893711.1), *Ctenopharyngodon idella* (grass carp, AOZ60534.1), *Cyprinus carpio* (common carp, CBX89936.1), *Scatophagus argus* (spotted scat, KU760724.1), *Danio rerio* (zebrafish, NP_775385.1), *Paralichthys olivaceus* (Japanese flounder, ADP09415.1), *Carassius auratus* (goldfish, CAD58853.1), *Dicentrarchus labrax* (European sea bass, CBN82190.1), *Takifugu rubripes* (fugu, NP_001027732.1), *Schizothorax prenanti* (Ya-fish, AGF80338.1), *Tetraodon nigroviridis* (spotted green pufferfish, AAQ55178.1), *Larimichthys crocea* (large yellow croaker, XP_010743320.1), *Verasper moseri* (barfin flounder, BAF64434.1), *Poecilia formosa* (Amazon molly, XP_007565095.1), *Takifugu porphyreus* (purple puffer, BAB71733.1), *Oncorhynchus mykiss* (rainbow trout, AAS45132.1), *Lepisosteus oculatus* (spotted gar, XP_006634516.1), *Xenopus tropicalis* (tropical clawed frog, XP_004915370.1), *Anser anser* (domestic goose, ABF19809.1), *Phaethon lepturus* (white-tailed tropicbird, XP_010285586.1), *Mus musculus* (house mouse, NP_058673.2), *Rattus norvegicus* (Norway rat, NP_037231.1), *Lipotes vexillifer* (Yangtze River dolphin, XP_007450183.1), *Orcinus orca* (killer whale, XP_004268107.1), *Pantholops hodgsonii* (chiru, XP_005972873.1), *Capra hircus* (goat, NP_001272520.1), *Bubalus bubalis* (water buffalo, XP_006046924.1), *Bos grunniens* (Tibetan yak, ADH51715.1), and *Gallus gallus* (chicken, AEP17334.1), and *Homo sapiens* (human, NP_005903.2).

extracellular, and intracellular loops. The PMY, DRY, and DPxxY motifs were predicted at homologous positions with MC4Rs of other species (Fig. 2). As shown in Figs. 1 and 2, the consensus sequence for protein kinase C phosphorylation ($Thr^{313}Phe^{314}Lys^{315}$) and the potential palmitoylation sites were found at C-terminus. Furthermore, the most conserved seven residues in each TMD were found in deduced grouper MC4R.

The cloned grouper *mrap2* consisted of a 696 bp ORF, encoding a putative protein of 232 amino acids with an estimated molecular mass of 26.43 kDa (Fig. 3). Similar to other MRAP2s, the grouper MRAP2 contained several features including a single TMD, a potential *N*-linked glycosylation site (Asn^{6}) within N-terminus, a putative motif (LKAHKYS) crucial for the formation of antiparallel homodimers (Sebag and Hinkle, 2009b), and a long C-terminal tail with many conserved residues (Supplementary Figure).

Phylogenetic tree analysis showed that both *Eco*MC4R and *Eco*MRAP2 were localized in a clade with homologs of other teleosts, respectively (Figs. 4 and 5). The identified *Eco*MC4R was nested with MC4Rs of large yellow croaker and spotted scat, European seabass and flounder (Fig. 4), while the *Eco*MRAP2 was nested with MRAP2 of black rockcod, amberjack and ballan wrasse (Fig. 5).

3.2. Tissue expression of grouper mc4r and mrap2

The qRT-PCR results showed that *mc4r* was highly expressed in the central nervous system, including olfactory bulb, mesencephalon, cerebellum, medulla and hypothalamus (Fig. 6A and 6B). Sexual dimorphism was observed in peripheral *mc4r* expression. In female grouper, *mc4r* was moderately expressed in pituitary gland, gill and spleen but not in other peripheral tissues studied such as ovary (Fig. 6B). In male grouper, *mc4r* was expressed more widely in the periphery, including liver, stomach, testis, kidney and spleen (Fig. 6A).

As shown in Fig. 6C and 6D, *mrap2* was highly expressed in central nervous system and testis (but not in ovary). Similar to the *mc4r* expression, *mrap2* was expressed more widely in the male than in the female in peripheral tissues. In female grouper, *mrap2* was primarily expressed in skin but not significantly in other peripheral tissues studied (Fig. 6D). In male grouper, *mrap2* was expressed more widely in the periphery, including stomach, testis, head kidney, kidney, skin, muscle and gill (Fig. 6C).

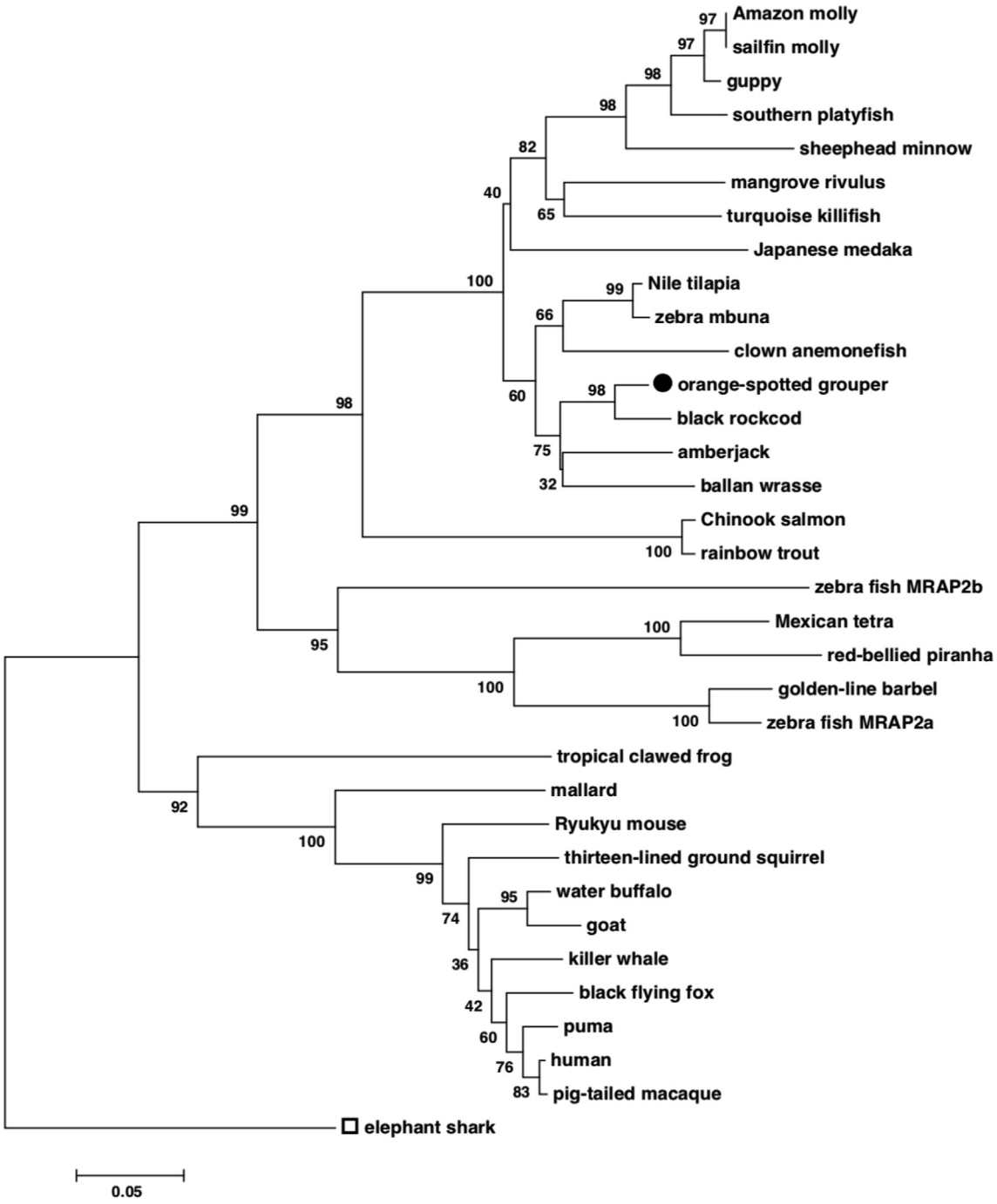

Fig. 5. Phylogenetic tree of MRAP2. The tree was constructed using the neighbor-joining (NJ) method. Numbers at nodes indicate the bootstrap value, as percentages, obtained for 1000 replicates. Black dot and open boxes shows *Eco*MRAP2 and outgroup, respectively. MRAP2s: *Epinephelus coioides* (orange-spotted grouper, MK425026), *Callorhinchus milii* (elephant shark, XP_007906624.1), *Danio rerio* (zebrafish, MRAP2a: P0DM64.1, and MRAP2b: F8W4H9.1), *Oreochromis niloticus* (Nile tilapia, XP_003458293.2), *Oryzias latipes* (Japanese medaka, XP_023809099.1), *Xiphophorus maculatus* (southern platyfish, XP_023203082.1), *Seriola lalandi dorsalis* (amberjack, XP_023270763.1), *Poecilia reticulata* (guppy, XP_008395815.1), *Nothobranchius furzeri* (turquoise killifish, XP_015802891.1), *Poecilia latipinna* (sailfin molly, XP_014898201.1), *Poecilia formosa* (Amazon molly, XP_007546516.2), *Notothenia coriiceps* (black rockcod, XP_010790801.1), *Kryptolebias marmoratus* (mangrove rivulus, XP_017267334.1), *Maylandia zebra* (zebra mbuna, XP_004568825.1), *Oncorhynchus tshawytscha* (Chinook salmon, XP_024278413.1), *Amphiprion ocellaris* (clown anemonefish, XP_023122806.1), *Astyanax mexicanus* (Mexican tetra, XP_007237340.2), *Oncorhynchus mykiss* (rainbow trout, XP_021467183.1), *Sinocyclocheilus grahami* (golden-line barbell, XP_016132131.1), *Cyprinodon variegatus* (sheephead minnow, XP_015225225.1), *Pygocentrus nattereri* (red-bellied piranha, XP_017562291.1), *Labrus bergylta* (ballan wrasse, XP_020497189.1), *Xenopus tropicalis* (tropical clawed frog, XP_002933963.1), *Anas platyrhynchos* (mallard, XP_021123507.1), *Ictidomys tridecemlineatus* (thirteen-lined ground squirrel, XP_021581743.1), *Mus caroli* (Ryukyu mouse, XP_021029091.1), *Capra hircus* (goat, XP_017908671.1), *Puma concolor* (puma, XP_025781535.1), *Bubalus bubalis* (water buffalo, XP_006054803.2), *Orcinus orca* (killer whale, XP_004270117.1), *Pteropus alecto* (black flying fox, XP_006926405.1), *Macaca nemestrina* (pig-tailed macaque, XP_011764298.1), and *Homo sapiens* (human, BC010003.2).

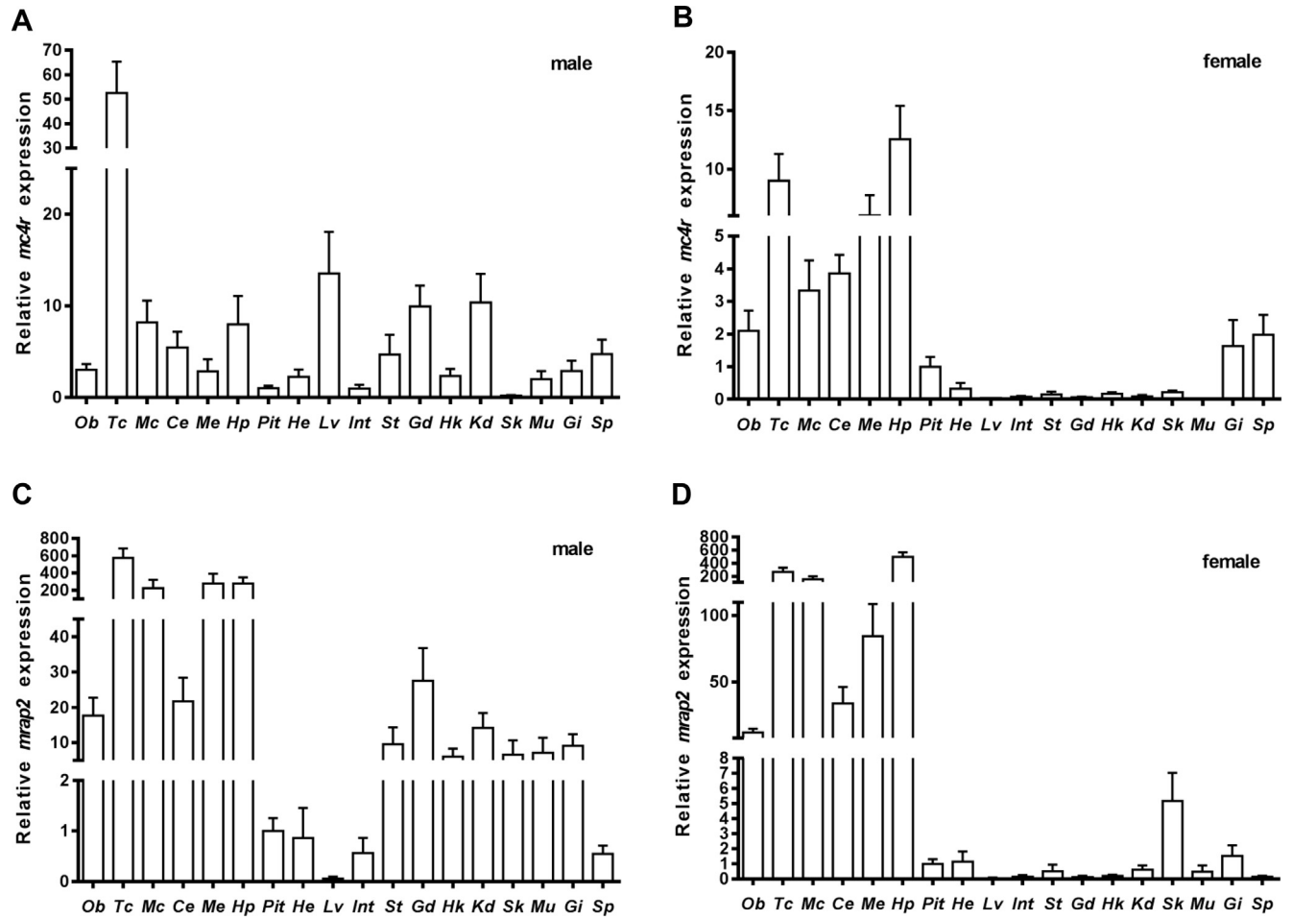

Fig. 6. Expression of *mc4r* (A, B) and *mrap2* (C, D) in grouper. The mRNA expressions of *mc4r* and *mrap2* were analyzed by qRT-PCR, and two reference genes, *β-actin* and *gapdh*, were used as double internal controls. The results were presented as the relative expression ratio of each target to reference genes. The mRNA relative expression was normalized as the fold of pituitary *mc4r* or *mrap2* expression. All data were expressed as the mean ± SEM (n = 6). Ob: olfactory bulb; Tc: telencephalon; Mc: mesencephalon; Ce: cerebellum; Me: medulla; Hp: hypothalamus; Pit: pituitary gland; He: heart; Lv: liver; Int: intestine; St: stomach; Gd: gonads; Hk: head kidney; Kd: kidney; Sk: skin; Mu: muscle; Gi: gill; Sp: spleen.

Table 2
Ligand binding properties of *Eco*MC4R.

MC4R	B_{max}	NDP-MSH IC_{50} (nM)	α-MSH IC_{50} (nM)	$ACTH_{(1–24)}$ IC_{50} (nM)
hMC4R	100	48.36 ± 3.49	445.97 ± 120.14	123.85 ± 24.28
*Eco*MC4R	41.52 ± 4.89[b]	2.54 ± 0.71[b]	95.18 ± 31.72[a]	42.50 ± 12.22[a]

Values are expressed as the mean ± S.E.M. of at least three independent experiments.
[a] : Significantly different from the parameter of hMC4R, $P < 0.05$ by Student *t* test.
[b] : Significantly different from the parameter of hMC4R, $P < 0.01$ by Student *t* test.

3.3. Ligand binding properties of EcoMC4R

Competitive ligand binding assays were performed to study the binding property of *Eco*MC4R. Different concentrations of unlabeled ligands including NDP-MSH, α-MSH, and ACTH (1–24), were used to compete with a fixed amount of radioligand ^{125}I-NDP-MSH. As shown in Table 2 and Fig. 7, the maximal binding of *Eco*MC4R was 41.52 ± 4.89% of that of the hMC4R (Table 2 and Fig. 7). *Eco*MC4R has significantly lower IC_{50} values when compared with hMC4R (Table 2). Similar to hMC4R, *Eco*MC4R bound to NDP-MSH with the highest affinity (IC_{50}, 2.54 ± 0.71 nM), followed by ACTH (1–24) (IC_{50}, 42.50 ± 12.22 nM) and α-MSH (IC_{50}, 95.18 ± 31.72 nM) (Table 2).

3.4. cAMP signaling properties of EcoMC4R

The signaling property of *Eco*MC4R was studied by cAMP RIA. As shown in Fig. 8, when stimulated by NDP-MSH, α-MSH or ACTH (1–24), *Eco*MC4R had dose-dependent increase of intracellular cAMP (Fig. 8). The basal signaling of *Eco*MC4R was 4.46 times that of hMC4R (Table 3 and Fig. 8). Similar maximal responses to NDP-MSH and α-MSH stimulation were observed between *Eco*MC4R and hMC4R, whereas *Eco*MC4R initiates significantly decreased maximal response to ACTH (1–24) stimulation (Table 3 and Fig. 8). The EC_{50}s of *Eco*MC4R are significantly lower than those of hMC4R (Table 3).

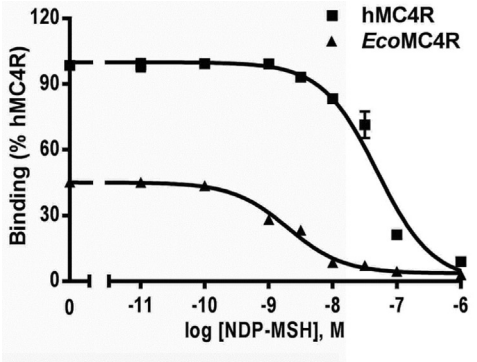

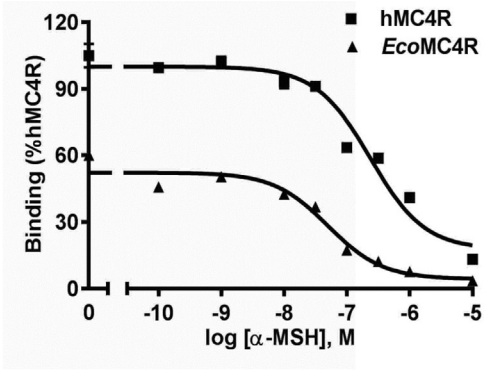

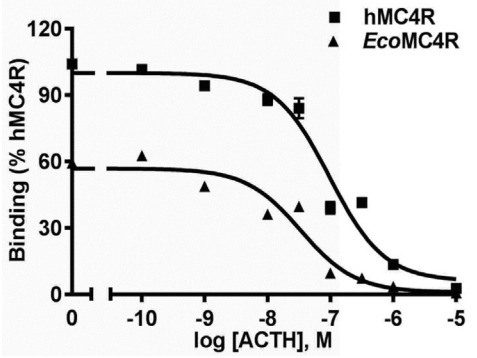

Fig. 7. Ligand binding properties of *Eco*MC4R. HEK293T cells were transiently transfected with hMC4R or *Eco*MC4R plasmids, and the binding properties were measured 48 h later by displacing the binding of ^{125}I-NDP-MSH using different concentrations of unlabeled NDP-, α-MSH, or ACTH (1–24). Data are expressed as % of hMC4R binding ± range from duplicate measurements within one experiment. The curves are representative of at least three independent experiments.

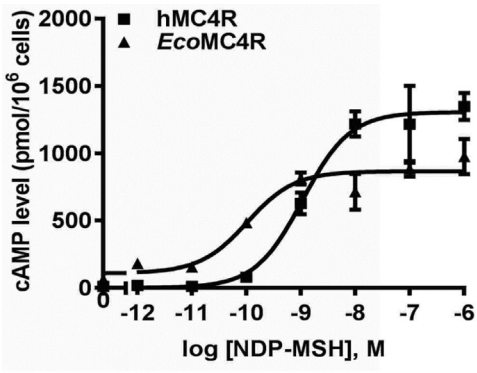

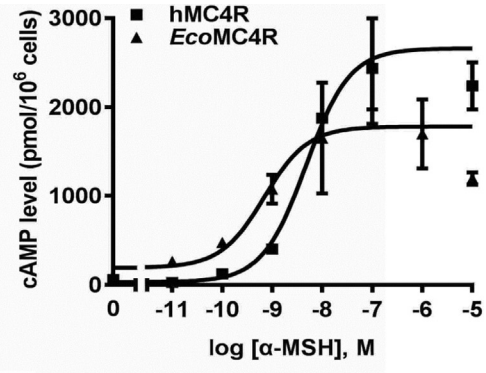

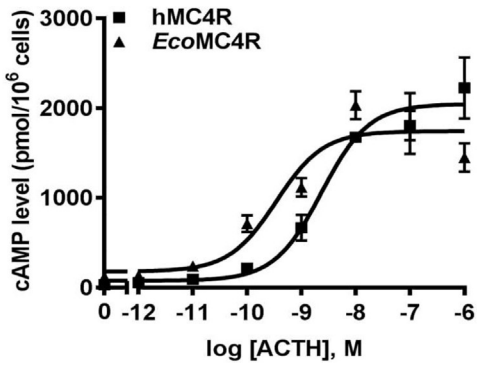

Fig. 8. Signaling properties of *Eco*MC4R. HEK293T cells were transiently transfected with hMC4R or *Eco*MC4R plasmids, and intracellular cAMP levels were measured by RIA after stimulation with different concentrations of NDP-, α-MSH or ACTH (1–24). Data are mean ± S.E.M from triplicate measurements within one experiment. All experiments were performed at least three times independently.

3.5. Modulation of EcoMC4R signaling by EcoMRAP2

To investigate potential modulation of *Eco*MC4R signaling by *Eco*MRAP2, cells were co-transected with MC4R and MRAP2 in different ratios. As shown in Fig. 9A, both basal and α-MSH-stimulated cAMP levels were significantly decreased when cells were co-transfected with 1:1, 1:3 or 1:5 (MC4R:MRAP2) compared with no MRAP2 was co-transfected.

When ERK1/2 phosphorylation was assessed, basal ERK1/2 activation is significantly increased by *Eco*MRAP2 dose-dependently, whereas ERK1/2 activation induced by 10^{-6} M α-MSH was not affected by *Eco*MRAP2 (Fig. 9B and C).

4. Discussion

To better understand the physiological roles of MC4R and potential modulation of its function by MRAP2 in orange-spotted grouper, we cloned grouper *mc4r* and *mrap2* cDNAs and investigated their tissue

Table 3
Signaling properties of *Eco*MC4R.

MC4R	Basal	NDP-MSH		α-MSH		$ACTH_{(1–24)}$	
		EC_{50} (nM)	Rmax (%)	EC_{50} (nM)	Rmax (%)	EC_{50} (nM)	Rmax (%)
hMC4R	100	0.95 ± 0.22	100	2.23 ± 0.38	100	4.25 ± 1.51	100
*Eco*MC4R	446.56 ± 64.31[c]	0.11 ± 0.02[b]	73.54 ± 19.72	0.46 ± 0.13[a]	84.46 ± 13.08	0.33 ± 0.12[a]	66.23 ± 11.09 [a]

Values are expressed as the mean ± S.E.M. of at least three independent experiments. The basal cAMP level of hMC4R was 30.13 ± 11.66 pmol/10^6 cells. The maximal responses (Rmax) of hMC4R were 1780.67 ± 350.19, 2471.40 ± 240.99, and 2578.67 ± 921.39 pmol/10^6 cells upon NDP-MSH, α-MSH and ACTH (1–24) stimulation, respectively.

[a] : Significantly different from the parameter of hMC4R, $P < 0.05$ by Student *t* test.
[b] : Significantly different from the parameter of hMC4R, $P < 0.01$ by Student *t* test.
[c] : Significantly different from the parameter of hMC4R, $P < 0.001$ by Student *t* test.

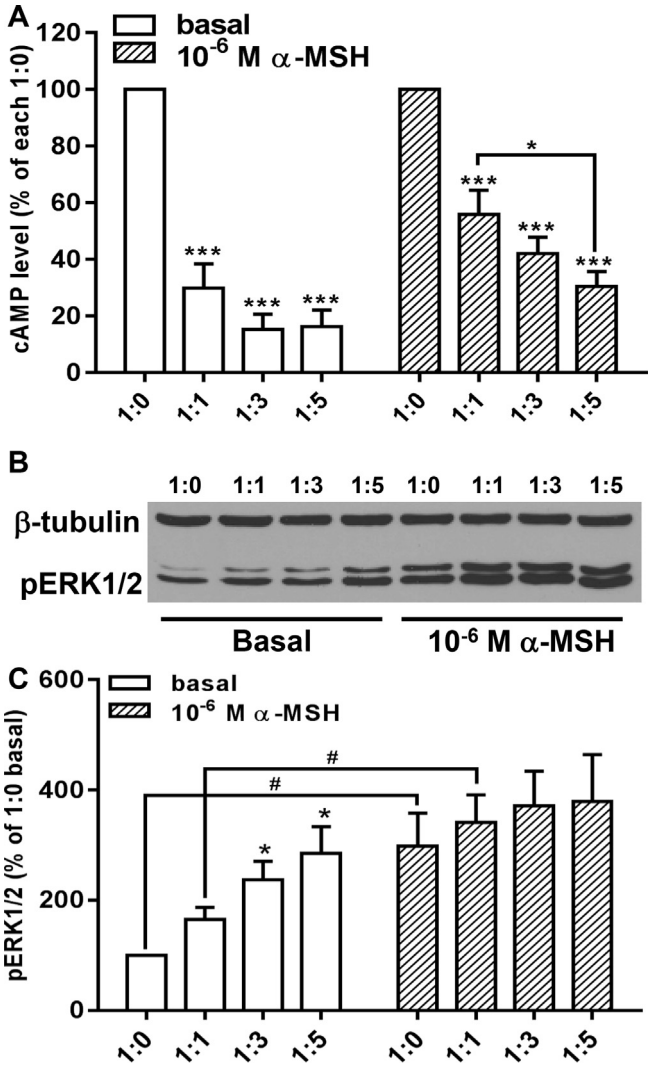

Fig. 9. Effects of MRAP2 on grouper MC4R signaling. HEK293T cells were co-transfected with *Eco*MC4R and *Eco*MRAP2 at four different ratios from 1:0 to 1:5 (MC4R/MRAP2). cAMP accumulation (A) and ERK1/2 phosphorylation (B & C) experiments were performed as described in *Materials and Methods*. (A) Basal and 10^{-6} M α-MSH stimulated cAMP accumulation. ***: $P < 0.001$ relative to 1:0 basal or stimulated cAMP activity, respectively; *: $P < 0.05$. Average value of 1:0 basal equals 178.61 ± 40.84; average value of 1:0 10^{-6} M α-MSH stimulated equals 1217.24 ± 130.88. (B, C) Western blot analysis for pERK1/2 after co-transfection. *: $P < 0.05$ relative to 1:0 basal; #: $P < 0.05$ significantly different between basal and 10^{-6} M α-MSH treated cells transfected with same plasmid ratios.

distribution. We also studied the pharmacological properties of grouper MC4R.

Phylogenetic analysis revealed that *Eco*MC4R clustered with teleost MC4Rs and nested with large yellow croaker MC4R (Fig. 4). The deduced amino acid sequence of the cloned grouper MC4R displayed several structural features similar as MC4Rs of other species, including seven TMDs, ECLs and ICLs (Figs. 1 and 3). The amino acid sequence of MC4R is highly conserved at seven hydrophobic TMDs that have been demonstrated to be crucial for ligand binding and activation (Yang et al., 2000; Tao, 2010). However, similar to other teleost MC4Rs, there was lower conservation in the ECLs and amino- and carboxyl-termini (Fig. 3) (Li et al., 2017). The conserved motifs and residues, such as PMY, DRY, DPxxY, and the most conserved residues in each TMD, which are known to be significant to maintain receptor structure and function, were also identified in *Eco*MC4R (Figs. 1 and 3). The C-terminal phosphorylation and palmitoylation sites were also conserved in grouper MC4R (Figs. 1 and 3).

The cloned grouper MRAP2 had a single highly conserved TMD and a potential *N*-linked glycosylation site at N-terminal domain, similar to MRAP2s of other species (Fig. 2 and Supplementary Figure). Furthermore, the LKAHKYS motif, crucial for the formation of antiparallel homodimers (Sebag and Hinkle, 2009b), was also conserved in grouper MRAP2. Phylogenetic analysis revealed that *Eco*MRAP2 was clustered with teleost MRAP2s, and nested with black rockcod, amberjack and ballan wrasse MRAP2s (Fig. 5).

As expected, *mc4r* was highly expressed in the central nervous system, consistent with its potential role in regulating energy homeostasis, especially in food intake (Fig. 6). In the periphery, *mc4r* was more widely expressed in the male than in the female, especially in testis (but not in ovary). The co-expression of *mc4r* with *mrap2* in the central nervous system indicates that MRAP2 might modulate MC4R signaling, hence altering MC4R-regulated physiological functions. The two genes were also co-expressed in the testis (but not ovary), suggesting that the MC4R might have differential roles in regulating gonadal function (Fig. 6).

To investigate the binding and signaling properties of *Eco*MC4R, three ligands were used in the present study, and hMC4R was employed herein for comparison. Binding experiments showed that the maximum binding capacity of *Eco*MC4R was about 40% of that of hMC4R (Fig. 7 and Table 2). Decreased binding capacity was also observed previously in spotted scat (Li et al., 2016), grass carp MC4R (Li et al., 2017), and swamp eel (Yi et al., 2018). *Eco*MC4R bound to NDP-MSH with an IC_{50} of 2.54 nM, ~20-fold lower than that of hMC4R. The IC_{50}s for α-MSH and ACTH (1–24) of *Eco*MC4R were ~5 and 3-fold lower than those of hMC4R, respectively (Fig. 7 and Table 2). Previous pharmacological assays demonstrated that in several teleosts, including fugu, trout, spotted scat, grass carp, and swamp eel, MC4Rs have high affinity for ACTH (Haitina et al., 2004; Klovins et al., 2004; Li et al., 2016; Li et al., 2017; Yi et al., 2018). Our results in grouper were consistent with those studies, lending further support for the hypothesis that ACTH is the original ligand for the MCRs (Metz et al., 2006).

We showed that of the three ligands studied, NDP-MSH was the most potent agonist for *Eco*MC4R with an EC_{50} of 0.11 nM (Table 3). Similar results were obtained in several other teleost MC4Rs, including grass carp, spotted scat, and swamp eel (Li et al., 2016; Li et al., 2017; Yi et al., 2018). Therefore, NDP-MSH can be a prospective ligand for experiments investigating the roles of MC4R in the regulation of teleost energy homeostasis.

We showed that *Eco*MC4R was constitutively active in Gs-cAMP pathway (Fig. 8). Previously, hMC4R has been shown to be constitutively active in Gs-cAMP signaling (Tao et al., 2010; Tao, 2014). Naturally occurring mutations in *MC4R* resulting in decreased constitutive activity are considered as a potential cause of human obesity (Srinivasan et al., 2004). Several studies demonstrated that some fish MC4Rs have much higher constitutive activity in Gs-cAMP signaling (Sanchez et al., 2009; Sebag et al., 2013; Li et al., 2016; Li et al., 2017; Yi et al., 2018). Constitutive activity in fish MC4R is potentially relevant for the adaptation to dark cave in Mexican cavefish (Aspiras et al., 2015). The potential relevance of constitutive activity in teleost MC4Rs in regulation of energy balance, especially in food intake, remains to be studied more extensively.

To investigate potential modulation of MC4R signaling by MRAP2, we co-transfected MC4R and MRAP2 in different ratios into HEK293T cells and then stimulated the cells with α-MSH. Our results showed that MRAP2 decreased basal and α-MSH-stimulated Gs-cAMP signaling but increased basal ERK1/2 signaling (Fig. 9). Due to the significantly increased basal ERK1/2 signaling when cells were co-transfected with higher ratio of *mrap2* (*mc4r*:*mrap2* at 1:3 or 1:5), no significant α-MSH-mediated stimulation in ERK1/2 could be measured (Fig. 9). Previous studied showed that MRAP2 decreases basal cAMP signaling in mouse MC4R but not in hMC4R (Chan et al., 2009; Asai et al., 2013; Kay et al., 2015) (reviewed in (Clark and Chan, 2017)). MRAP2 increases cAMP response to α-MSH stimulation (Asai et al., 2013). In zebrafish, MRAP2a decreases both basal and α-MSH-stimulated cAMP generation (but increases the responsiveness to ACTH stimulation) whereas MRAP2b decreases basal cAMP level but does not decrease maximal signaling initiated by α-MSH (Josep Agulleiro et al., 2013; Sebag et al., 2013). There is no report of MRAP2 effect on ERK1/2 signaling. Therefore, MRAP2 has different effects on MC4R signaling in different species.

In summary, we cloned *mc4r* and *mrap2* from orange-spotted grouper and shown these genes to be evolutionarily conserved. Both genes were highly expressed in the central nervous system. Grouper MC4R had high constitutive activity, and respond to several agonists with higher potency than hMC4R. Grouper MRAP2 decreased basal and agonist-stimulated cAMP signaling but increased basal ERK1/2 signaling, suggesting that MRAP2 had differential effects on cAMP and ERK1/2 signaling pathways. The *in vivo* relevance of these modulations by MRAP2 on MC4R physiology in grouper remains to be studied.

Declaration of Competing Interest

The authors declare that they have no known competing financial interests or personal relationships that could have appeared to influence the work reported in this paper.

Acknowledgments

This research was supported by the Science and Technology Planning Project of Guangdong Province (2014A020208136, 2018A03027), the Key Science Project of Lingnan Normal University (LZL1508), the Overseas Scholarship Program for Elite Young and Middle-aged Teachers of Lingnan Normal University, Guangdong Provincial Natural Science Foundation (2018B030311026), the Special Fund for Fisheries-Scientific Research of Guangdong Province (2018-04), and Science and Technology Planning Project of Guangzhou (201804020013), the Special Fund for Fisheries-Scientific Research of Guangdong Province (SDYY-2018-04), Guangdong Provincial Special Fund for Modern Agriculture Industry Technology Innovation Teams and Guangdong Provincial Special Fund For Science and Technology Planning Project of Jieyang (2060302). This study was also partially supported by Animal Health and Disease Research Program of College of Veterinary Medicine at Auburn University.

Appendix A. Supplementary data

Supplementary data to this article can be found online at https://doi.org/10.1016/j.ygcen.2019.113234.

References

Asai, M., Ramachandrappa, S., Joachim, M., Shen, Y., Zhang, R., Nuthalapati, N., Ramanathan, V., Strochlic, D.E., Ferket, P., Linhart, K., et al., 2013. Loss of function of the melanocortin 2 receptor accessory protein 2 is associated with mammalian obesity. Science 341, 275–278.

Aspiras, A.C., Rohner, N., Martineau, B., Borowsky, R.L., Tabin, C.J., 2015. Melanocortin 4 receptor mutations contribute to the adaptation of cavefish to nutrient-poor conditions. Proc. Natl. Acad. Sci. U.S.A. 112, 9668–9673.

Balthasar, N., Dalgaard, L.T., Lee, C.E., Yu, J., Funahashi, H., Williams, T., Ferreira, M., Tang, V., McGovern, R.A., Kenny, C.D., et al., 2005. Divergence of melanocortin pathways in the control of food intake and energy expenditure. Cell 123, 493–505.

Breit, A., Wolff, K., Kalwa, H., Jarry, H., Buch, T., Gudermann, T., 2006. The natural inverse agonist agouti-related protein induces arrestin-mediated endocytosis of melanocortin-3 and -4 receptors. J. Biol. Chem. 281, 37447–37456.

Bustin, S.A., Benes, V., Garson, J.A., Hellemans, J., Huggett, J., Kubista, M., Mueller, R., Nolan, T., Pfaffl, M.W., Shipley, G.L., et al., 2009. The MIQE guidelines: minimum information for publication of quantitative real-time PCR experiments. Clin. Chem. 55, 611–622.

Cerda-Reverter, J.M., Ringholm, A., Schioth, H.B., Peter, R.E., 2003. Molecular cloning, pharmacological characterization, and brain mapping of the melanocortin 4 receptor in the goldfish: involvement in the control of food intake. Endocrinology 144, 2336–2349.

Chan, L.F., Webb, T.R., Chung, T.T., Meimaridou, E., Cooray, S.N., Guasti, L., Chapple, J.P., Egertova, M., Elphick, M.R., Cheetham, M.E., et al., 2009. MRAP and MRAP2 are bidirectional regulators of the melanocortin receptor family. Proc. Natl. Acad. Sci. U.S.A. 106, 6146–6151.

Chen, C., Okayama, H., 1987. High-efficiency transformation of mammalian cells by plasmid DNA. Mol. Cell. Biol. 7, 2745–2752.

Chen, T., Tang, Z.G., Yan, A.F., Li, W.S., Lin, H.R., 2008. Molecular cloning and mRNA expression analysis of two GH secretagogue receptor transcripts in orange-spotted grouper (*Epinephelus coioides*). J. Endocrinol. 199, 253–265.

Clark, A.J., Chan, L.F., 2017. Promiscuity among the MRAPs. J. Mol. Endocrinol. 58, F1–F4.

Daniels, D., Patten, C.S., Roth, J.D., Yee, D.K., Fluharty, S.J., 2003. Melanocortin receptor signaling through mitogen-activated protein kinase in vitro and in rat hypothalamus. Brain Res. 986, 1–11.

Dores, R.M., Garcia, Y., 2015. Views on the co-evolution of the melanocortin-2 receptor, MRAPs, and the hypothalamus/pituitary/adrenal-interrenal axis. Mol. Cell. Endocrinol. 408, 12–22.

Farooqi, I.S., Keogh, J.M., Yeo, G.S., Lank, E.J., Cheetham, T., O'Rahilly, S., 2003. Clinical spectrum of obesity and mutations in the melanocortin 4 receptor gene. N. Engl. J. Med. 348, 1085–1095.

Gantz, I., Miwa, H., Konda, Y., Shimoto, Y., Tashiro, T., Watson, S.J., DelValle, J., Yamada, T., 1993. Molecular cloning, expression, and gene localization of a fourth melanocortin receptor. J. Biol. Chem. 268, 15174–15179.

Haitina, T., Klovins, J., Andersson, J., Fredriksson, R., Lagerstrom, M.C., Larhammar, D., Larson, E.T., Schioth, H.B., 2004. Cloning, tissue distribution, pharmacology and three-dimensional modelling of melanocortin receptors 4 and 5 in rainbow trout suggest close evolutionary relationship of these subtypes. Biochem. J. 380, 475–486.

He, S., Tao, Y.X., 2014. Defect in MAPK signaling as a cause for monogenic obesity caused by inactivating mutations in the melanocortin-4 receptor gene. Int. J. Biol. Sci. 10, 1128–1137.

Hinney, A., Volckmar, A.L., Knoll, N., 2013. Melanocortin-4 receptor in energy homeostasis and obesity pathogenesis. Prog. Mol. Biol. Transl. Sci. 114, 147–191.

Huang, H., Tao, Y.X., 2012. Pleiotropic functions of the transmembrane domain 6 of human melanocortin-4 receptor. J. Mol. Endocrinol. 49, 237–248.

Huszar, D., Lynch, C.A., Fairchild-Huntress, V., Dunmore, J.H., Fang, Q., Berkemeier, L.R., Gu, W., Kesterson, R.A., Boston, B.A., Cone, R.D., et al., 1997. Targeted disruption of the melanocortin-4 receptor results in obesity in mice. Cell 88, 131–141.

Josep Agulleiro, M., Cortes, R., Fernandez-Duran, B., Navarro, S., Guillot, R., Meimaridou, E., Clark, A.J., Cerda-Reverter, J.M., 2013. Melanocortin 4 receptor becomes an ACTH receptor by coexpression of melanocortin receptor accessory protein 2. Mol. Endocrinol. 27, 1934–1945.

Kay, E.I., Botha, R., Montgomery, J.M., Mountjoy, K.G., 2015. hMRAPα, but not hMRAP2, enhances hMC4R constitutive activity in HEK293 cells and this is not dependent on hMRAPα induced changes in hMC4R complex N-linked glycosylation. PLoS One 10, e0140320.

Klovins, J., Haitina, T., Fridmanis, D., Kilianova, Z., Kapa, I., Fredriksson, R., Gallo-Payet,

N., Schioth, H.B., 2004. The melanocortin system in Fugu: determination of POMC/AGRP/MCR gene repertoire and synteny, as well as pharmacology and anatomical distribution of the MCRs. Mol. Biol. Evol. 21, 563–579.
Li, J.T., Yang, Z., Chen, H.P., Zhu, C.H., Deng, S.P., Li, G.L., Tao, Y.X., 2016. Molecular cloning, tissue distribution, and pharmacological characterization of melanocortin-4 receptor in spotted scat, *Scatophagus argus*. Gen. Comp. Endocrinol. 230–231, 143–152.
Li, L., Yang, Z., Zhang, Y.P., He, S., Liang, X.F., Tao, Y.X., 2017. Molecular cloning, tissue distribution, and pharmacological characterization of melanocortin-4 receptor in grass carp (*Ctenopharyngodon idella*). Domest. Anim. Endocrinol. 59, 140–151.
Livak, K.J., Schmittgen, T.D., 2001. Analysis of relative gene expression data using real-time quantitative PCR and the 2-ΔΔCT method. Methods 25, 402–408.
Metherell, L.A., Chapple, J.P., Cooray, S., David, A., Becker, C., Ruschendorf, F., Naville, D., Begeot, M., Khoo, B., Nurnberg, P., et al., 2005. Mutations in MRAP, encoding a new interacting partner of the ACTH receptor, cause familial glucocorticoid deficiency type 2. Nat. Genet. 37, 166–170.
Metz, J.R., Peters, J.J., Flik, G., 2006. Molecular biology and physiology of the melanocortin system in fish: a review. Gen. Comp. Endocrinol. 148, 150–162.
Mo, X.L., Tao, Y.X., 2013. Activation of MAPK by inverse agonists in six naturally occurring constitutively active mutant human melanocortin-4 receptors. Biochim. Biophys. Acta, Mol. Basis Dis. 1832, 1939–1948.
Mo, X.L., Yang, R., Tao, Y.X., 2012. Functions of transmembrane domain 3 of human melanocortin-4 receptor. J. Mol. Endocrinol. 49, 221–235.
Mountjoy, K.G., Mortrud, M.T., Low, M.J., Simerly, R.B., Cone, R.D., 1994. Localization of the melanocortin-4 receptor (MC4-R) in neuroendocrine and autonomic control circuits in the brain. Mol. Endocrinol. 8, 1298–1308.
Nickolls, S.A., Fleck, B., Hoare, S.R., Maki, R.A., 2005. Functional selectivity of melanocortin 4 receptor peptide and nonpeptide agonists: evidence for ligand-specific conformational states. J. Pharmacol. Exp. Ther. 313, 1281–1288.
Novoselova, T.V., Larder, R., Rimmington, D., Lelliott, C., Wynn, E.H., Gorrigan, R.J., Tate, P.H., Guasti, L., O'Rahilly, S., Clark, A.J.L., 2016. Loss of Mrap2 is associated with Sim1 deficiency and increased circulating cholesterol. J. Endocrinol. 230, 13–26.
Palczewski, K., Kumasaka, T., Hori, T., Behnke, C.A., Motoshima, H., Fox, B.A., Le Trong, I., Teller, D.C., Okada, T., Stenkamp, R.E., 2000. Crystal structure of rhodopsin: A G protein-coupled receptor. Science 289, 739–745.
Saitou, N., Nei, M., 1987. The neighbor-joining method: a new method for reconstructing phylogenetic trees. Mol. Biol. Evol. 4, 406–425.
Sanchez, E., Rubio, V.C., Thompson, D., Metz, J., Flik, G., Millhauser, G.L., Cerda-Reverter, J.M., 2009. Phosphodiesterase inhibitor-dependent inverse agonism of agouti-related protein on melanocortin 4 receptor in sea bass (*Dicentrarchus labrax*). Am. J. Physiol. Regul., Integr. Compar. Physiol. 296, R1293–R1306.
Sebag, J.A., Hinkle, P.M., 2007. Melanocortin-2 receptor accessory protein MRAP forms antiparallel homodimers. Proc Natl Acad Sci U S A 104, 20244–20249.
Sebag, J.A., Hinkle, P.M., 2009a. Opposite effects of the melanocortin-2 (MC2) receptor accessory protein MRAP on MC2 and MC5 receptor dimerization and trafficking. J. Biol. Chem. 284, 22641–22648.
Sebag, J.A., Hinkle, P.M., 2009b. Regions of melanocortin 2 (MC2) receptor accessory protein necessary for dual topology and MC2 receptor trafficking and signaling. J. Biol. Chem. 284, 610–618.
Sebag, J.A., Hinkle, P.M., 2010. Regulation of G protein-coupled receptor signaling: specific dominant-negative effects of melanocortin 2 receptor accessory protein 2. Sci Signal 3, ra28.
Sebag, J.A., Zhang, C., Hinkle, P.M., Bradshaw, A.M., Cone, R.D., 2013. Developmental control of the melanocortin-4 receptor by MRAP2 proteins in zebrafish. Science 341, 278–281.
Song, Y., Cone, R.D., 2007. Creation of a genetic model of obesity in a teleost. FASEB J. 21, 2042–2049.
Srinivasan, S., Lubrano-Berthelier, C., Govaerts, C., Picard, F., Santiago, P., Conklin, B.R., Vaisse, C., 2004. Constitutive activity of the melanocortin-4 receptor is maintained by its N-terminal domain and plays a role in energy homeostasis in humans. J. Clin. Invest. 114, 1158–1164.
Steiner, A.L., Kipnis, D.M., Utiger, R., Parker, C., 1969. Radioimmunoassay for the measurement of adenosine 3',5'-cyclic phosphate. Proc. Natl. Acad. Sci. U.S.A. 64, 367–373.
Sutton, G.M., Duos, B., Patterson, L.M., Berthoud, H.R., 2005. Melanocortinergic modulation of cholecystokinin-induced suppression of feeding through extracellular signal-regulated kinase signaling in rat solitary nucleus. Endocrinology 146, 3739–3747.
Tao, Y.X., 2009. Mutations in melanocortin-4 receptor and human obesity. Prog. Mol. Biol. Transl. Sci. 88, 173–204.
Tao, Y.X., 2010. The melanocortin-4 receptor: physiology, pharmacology, and pathophysiology. Endocr. Rev. 31, 506–543.
Tao, Y.X., 2014. Constitutive activity in melanocortin-4 receptor: biased signaling of inverse agonists. Adv. Pharmacol. 70, 135–154.
Tao, Y.X., Huang, H., Wang, Z.Q., Yang, F., Williams, J.N., Nikiforovich, G.V., 2010. Constitutive activity of neural melanocortin receptors. Methods Enzymol. 484, 267–279.
Tao, Y.X., Segaloff, D.L., 2003. Functional characterization of melanocortin-4 receptor mutations associated with childhood obesity. Endocrinology 144, 4544–4551.
Tao, Y.X., Segaloff, D.L., 2005. Functional analyses of melanocortin-4 receptor mutations identified from patients with binge eating disorder and nonobese or obese subjects. J. Clin. Endocrinol. Metab. 90, 5632–5638.
Valsalan, R., Krishnan, A., Almen, M.S., Fredriksson, R., Schioth, H.B., 2013. Early vertebrate origin of melanocortin 2 receptor accessory proteins (MRAPs). Gen. Comp. Endocrinol. 188, 123–132.
Västermark, Å., Schiöth, H.B., 2011. The early origin of melanocortin receptors, agouti-related peptide, agouti signalling peptide, and melanocortin receptor-accessory proteins, with emphasis on pufferfishes, elephant shark, lampreys, and amphioxus. Eur. J. Pharmacol. 660, 61–69.
Vongs, A., Lynn, N.M., Rosenblum, C.I., 2004. Activation of MAP kinase by MC4-R through PI3 kinase. Regul. Pept. 120, 113–118.
Wang, F., Chen, W., Lin, H.R., Li, W.S., 2014. Cloning, expression, and ligand-binding characterization of two neuropeptide Y receptor subtypes in orange-spotted grouper, *Epinephelus coioides*. Fish Physiol. Biochem. 40, 1693–1707.
Wei, R., Yuan, D., Zhou, C., Wang, T., Lin, F., Chen, H., Wu, H., Xin, Z., Yang, S., Chen, D., et al., 2013. Cloning, distribution and effects of fasting status of melanocortin 4 receptor (MC4R) in *Schizothorax prenanti*. Gene 532, 100–107.
Yang, L.K., Tao, Y.X., 2017. Biased signaling at neural melanocortin receptors in regulation of energy homeostasis. Biochim. Biophys. Acta, Mol. Basis Dis. 1863, 2486–2495.
Yang, Y.K., Fong, T.M., Dickinson, C.J., Mao, C., Li, J.Y., Tota, M.R., Mosley, R., Van Der Ploeg, L.H., Gantz, I., 2000. Molecular determinants of ligand binding to the human melanocortin-4 receptor. Biochemistry 39, 14900–14911.
Yi, T.L., Yang, L.K., Ruan, G.L., Yang, D.Q., Tao, Y.X., 2018. Melanocortin-4 receptor in swamp eel (*Monopterus albus*): cloning, tissue distribution, and pharmacology. Gene 678, 79–89.
Zhang, W.M., Zhang, L.H., Ma, G.Z., Zhang, Y., 2003. Cloning and sequence analysis of proipiomelanocortin (POMC) in orange-spotted grouper, *Epinephelus coioides*. Acta Hydrobiol. Sin. 27, 625–630.